A Non-blind Color Image Watermarking Scheme Resistent Against Geometric Attacks

Abdul GHAFOOR, Muhammad IMRAN

Department of Electrical Engineering, Military College of Signals,
National University of Sciences and Technology (NUST), Islamabad, Pakistan

abdulghafoor-mcs@nust.edu.pk, imran.muet@gmail.com

Abstract. *A non-blind color image watermarking scheme using principle component analysis, discrete wavelet transform and singular value decomposition is proposed. The color components are uncorrelated using principle component analysis. The watermark is embedded into the singular values of discrete wavelet transformed sub-band associated with principle component containing most of the color information. The scheme was tested against various attacks (including histogram equalization, rotation, Gaussian noise, scaling, cropping, Y-shearing, X-shearing, median filtering, affine transformation, translation, salt & pepper, sharpening), to check robustness. The results of proposed scheme are compared with state-of-the-art existing color watermarking schemes using normalized correlation coefficient and peak signal to noise ratio. The simulation results show that proposed scheme is robust and imperceptible.*

Keywords

Copyright protection, digital watermarking, principle component analysis, discrete wavelet transform, singular value decomposition, color watermarking.

1. Introduction

Digital data (such as images, audio and video) is widely available online. Multiple copies of original data can be made easily and it is difficult to distinguish between original and copied data. This creates the problem of owner identification, authentication and copyright protection. Watermarking is a possible solution [1]-[9].

In digital watermarking some information (images, audio, video) can be embedded into the data in such a way that it is not perceptible to human eye. This hidden data can later be extracted to prove the ownership [1], [3]. The quality of watermarking scheme is primarily based on two conflicting requirements, robustness (measured using normalized correlation coefficient (NC)) and imperceptibility (measured using peak signal to noise ratio (PSNR)) [1], [10].

Based on the domain, watermarking can be classified into spatial and frequency [4], [5], [9], [11], [12]. In spatial domain (generaly less complex, less robust and less secure [4], [5], [9], [13]), the pixel values of cover image are directly modified for watermark embedding [5]. In frequency domain (relatively robust, secure and imperceptible [4], [5], [9]), the cover image is transformed to other domain (using discrete cosine transform (DCT), discrete wavelet transform (DWT), discrete fourier transform (DFT) [5], [9], [12]) for watermark embedding [9].

Most of the image watermarking schemes are applicable [3] for gray level images and some schemes are related to color images. Out of color image watermarking schemes, [5], [6], [13] uses DWT and singular value decomposition (SVD) whereas [15] uses DWT and [16] uses SVD for watermark embedding.

In RGB images, R, G and B channels are highly correlated [6], [12], [13], and for quality watermarking (to improve imperceptibility) it is desirable that these channels are uncorrelated. [6] uses YUV color space and [13] uses YIQ color space to uncorrelate R, G and B channels.

Since [16] do not uncorrelate the R, G and B channels for watermark embedding, therefore the quality of watermarked image is not satisfactory. Moreover, [16] works in the spatial domain only, therefore it is not secure as compared to its frequency domain counterparts [4], [5], [9].

In the proposed non-blind color image watermarking scheme, the drawbacks of [16] are overcome. We use principle component analysis (PCA) to uncorrelate R, G and B channels. Since most of the information of color image is contained in first principle component [17], therefore first principle component is used for watermark embedding. Second level DWT of first principle component is performed and watermark is embedded by modifying the singular values of each band. Reverse process is applied for watermark extraction. The results of proposed scheme are compared with state-of-the-art existing color watermarking schemes using NC and PSNR. The simulation results show that proposed scheme is robust (against attacks like histogram equalization, rotation, Gaussian noise, scaling, cropping, Y-shearing, X-shearing, median filtering, affine transformation, translation, salt & pepper, sharpening) and imperceptible.

2. Color Image Watermarking Scheme

2.1 Watermark Embedding

Let the original color image I, is decomposed into its three components (R, G and B), where

$$R = \begin{pmatrix} r_{11} & r_{12} & \dots & r_{1N} \\ r_{21} & r_{22} & \dots & r_{2N} \\ \vdots & \vdots & \ddots & \vdots \\ r_{M1} & r_{M2} & \dots & r_{MN} \end{pmatrix},$$

$$G = \begin{pmatrix} g_{11} & g_{12} & \dots & g_{1N} \\ g_{21} & g_{22} & \dots & g_{2N} \\ \vdots & \vdots & \ddots & \vdots \\ g_{M1} & g_{M2} & \dots & g_{MN} \end{pmatrix},$$

$$B = \begin{pmatrix} b_{11} & b_{12} & \dots & b_{1N} \\ b_{21} & b_{22} & \dots & b_{2N} \\ \vdots & \vdots & \ddots & \vdots \\ b_{M1} & b_{M2} & \dots & b_{MN} \end{pmatrix},$$

M and N define the size of the original image.

Let a covariance matrix C be computed as

$$C = \frac{1}{MN}(AA^T) = Q\Lambda Q^{-1}$$

where

$$A = \begin{pmatrix} r_{11} \dots r_{1N} \; r_{21} \dots r_{2N} \dots r_{M1} \dots r_{MN} \\ g_{11} \dots g_{1N} \; g_{21} \dots g_{2N} \dots g_{M1} \dots g_{MN} \\ b_{11} \dots b_{1N} \; b_{21} \dots b_{2N} \dots b_{M1} \dots b_{MN} \end{pmatrix},$$

$$Q = \begin{pmatrix} q_{11} \; q_{12} \; q_{13} \\ q_{21} \; q_{22} \; q_{23} \\ q_{31} \; q_{32} \; q_{33} \end{pmatrix}, \qquad \Lambda = \begin{pmatrix} \lambda_{11} & 0 & 0 \\ 0 & \lambda_{22} & 0 \\ 0 & 0 & \lambda_{33} \end{pmatrix}$$

and $\lambda_{11} \geq \lambda_{22} \geq \lambda_{33}$. The principle components [18] of matrix C are written as

$$P = \begin{pmatrix} P_r \\ P_g \\ P_b \end{pmatrix} = Q^T A$$

$$= \begin{pmatrix} pr_{11} \dots pr_{1N} \; pr_{21} \dots pr_{2N} \dots pr_{M1} \dots pr_{MN} \\ pg_{11} \dots pg_{1N} \; pg_{21} \dots pg_{2N} \dots pg_{M1} \dots pg_{MN} \\ pb_{11} \dots pb_{1N} \; pb_{21} \dots pb_{2N} \dots pb_{M1} \dots pb_{MN} \end{pmatrix}.$$

Remark 1: Since R, G and B components are highly correlated [6], [12], [13], the PCA [17] is used here to uncorrelate these R, G and B components. The first component of PCA (P_r) contains most of the image information [17].

Let matrix

$$Prn = \begin{pmatrix} pr_{11} & pr_{12} & \dots & pr_{1N} \\ pr_{21} & pr_{22} & \dots & pr_{2N} \\ \vdots & \vdots & \ddots & \vdots \\ pr_{M1} & pr_{M2} & \dots & pr_{MN} \end{pmatrix}$$

be decomposed into its sub-bands using DWT (Haar) as following:

$$\begin{aligned} \begin{pmatrix} LL_1 & LH_1 & HL_1 & HH_1 \end{pmatrix} &= DWT(P_{rn}), \\ \begin{pmatrix} LL_2 & LH_2 & HL_2 & HH_2 \end{pmatrix} &= DWT(LL_1). \end{aligned}$$

Remark 2: In [15], various DWT families (like Haar, Daubechies, BiorSplines, ReverseBior, Symlets, and Coiflets) were explored for watermarking and performance of Haar was found better.

Remark 3: Since P_{rn} is composed of components from P_r and contains most of the color image information, therefore it is chosen for watermark embedding.

Remark 4: The use of DWT here is to improve the security level and robustness [5], [11]. The improvement in the security level and robustness is due to irregular distribution of watermark over the image during the inverse transform.

Let us decompose second level sub-bands using SVD [19] as follows:

$$\begin{aligned} LL_2 &= U_1 S_1 V_1^T, \\ LH_2 &= U_2 S_2 V_2^T, \\ HL_2 &= U_3 S_3 V_3^T, \\ HH_2 &= U_4 S_4 V_4^T \end{aligned}$$

where S_1, S_2, S_3 and S_4 are diagonal matrices and contain singular values in descending order. U_1, U_2, U_3, U_4, V_1, V_2, V_3 and V_4 are orthogonal matrices containing singular vectors.

Remark 5: Small perturbation in image does not cause large variation in singular values [3]-[6], [12].

Remark 6: Singular values own intrinsic properties of image (i.e. luminance information is contained in singular values, whereas geometric information is maintained by corresponding singular vectors) [1], [3]-[6] [11], [20].

The watermark is introduced as follows:

$$\begin{aligned} S_1 + \alpha W &= U_{w1} S_{w1} V_{w1}^T, \qquad (1) \\ S_2 + \alpha(\frac{W}{2}) &= U_{w2} S_{w2} V_{w2}^T, \\ S_3 + \alpha(\frac{W}{2}) &= U_{w3} S_{w3} V_{w3}^T, \\ S_4 + \alpha W &= U_{w4} S_{w4} V_{w4}^T \end{aligned}$$

where S_{w1}, S_{w2}, S_{w3} and S_{w4} are diagonal matrices and contain singular values in descending order, W is the watermark and α defines the strength factor.

Remark 7: If the size of singular values matrix and watermark matrix mismatch in (1), the watermark may be interpolated or decimated accordingly and reverse process applies for watermark extraction.

Let the modified sub-bands be as follows:

$$\begin{aligned} LL_w &= U_1 S_{w1} V_1^T, \\ LH_w &= U_2 S_{w2} V_2^T, \\ HL_w &= U_3 S_{w3} V_3^T, \\ HH_w &= U_4 S_{w4} V_4^T. \end{aligned}$$

The modified principle components are obtained as

$$P_w = \begin{pmatrix} P_{rw} \\ P_g \\ P_b \end{pmatrix} = \begin{pmatrix} prw_{11} \ldots prw_{1N} & prw_{21} \ldots prw_{2N} & \ldots prw_{M1} \ldots prw_{MN} \\ pg_{11} \ldots pg_{1N} & pg_{21} \ldots pg_{2N} & \ldots pg_{M1} \ldots pg_{MN} \\ pb_{11} \ldots pb_{1N} & pb_{21} \ldots pb_{2N} & \ldots pb_{M1} \ldots pb_{MN} \end{pmatrix}$$

where

$$\begin{pmatrix} prw_{11} & prw_{12} & \ldots & prw_{1N} \\ prw_{21} & prw_{22} & \ldots & prw_{2N} \\ \vdots & \vdots & \ddots & \vdots \\ prw_{M1} & prw_{M2} & \ldots & prw_{MN} \end{pmatrix} = IDWT(LL_w,\ LH_w,\ HL_w,\ HH_w).$$

The matrix A_w is obtained as

$$A_w = QP_w = \begin{pmatrix} rw_{11} \ldots rw_{1N} & rw_{21} \ldots rw_{2N} & \ldots rw_{M1} \ldots rw_{MN} \\ g_{11} \ldots g_{1N} & g_{21} \ldots g_{2N} & \ldots g_{M1} \ldots g_{MN} \\ b_{11} \ldots b_{1N} & b_{21} \ldots b_{2N} & \ldots b_{M1} \ldots b_{MN} \end{pmatrix}.$$

The watermarked image I_w is composed from (R_w, G, B) where

$$R_w = \begin{pmatrix} rw_{11} & rw_{12} & \ldots & rw_{1N} \\ rw_{21} & rw_{22} & \ldots & rw_{2N} \\ \vdots & \vdots & \ddots & \vdots \\ rw_{M1} & rw_{M2} & \ldots & rw_{MN} \end{pmatrix}.$$

2.2 Watermark Extraction

The received watermarked image $\hat{I_w}$ may be subject to perturbation (and attacks) on the watermarked image I_w.

Let $\hat{I}_w$ be decomposed into its components ($\hat{R}_w$, $\hat{G}$, $\hat{B}$), where

$$\hat{R_w} = \begin{pmatrix} \hat{r}w_{11} & \hat{r}w_{12} & \ldots & \hat{r}w_{1N} \\ \hat{r}w_{21} & \hat{r}w_{22} & \ldots & \hat{r}w_{2N} \\ \vdots & \vdots & \ddots & \vdots \\ \hat{r}w_{M1} & \hat{r}w_{M2} & \ldots & \hat{r}w_{MN} \end{pmatrix},$$

$$\hat{G} = \begin{pmatrix} \hat{g}_{11} & \hat{g}_{12} & \cdots & \hat{g}_{1N} \\ \hat{g}_{21} & \hat{g}_{22} & \cdots & \hat{g}_{2N} \\ \vdots & \vdots & \ddots & \vdots \\ \hat{g}_{M1} & \hat{g}_{M2} & \cdots & g_{MN} \end{pmatrix},$$

$$\hat{B} = \begin{pmatrix} \hat{b}_{11} & \hat{b}_{12} & \ldots & \hat{b}_{1N} \\ \hat{b}_{21} & \hat{b}_{22} & \ldots & \hat{b}_{2N} \\ \vdots & \vdots & \ddots & \vdots \\ \hat{b}_{M1} & \hat{b}_{M2} & \ldots & \hat{b}_{MN} \end{pmatrix}.$$

Let covariance matrix $\hat{C}$ be computed as

$$\hat{C} = \frac{1}{MN}(\hat{A}\hat{A}^T) = \hat{Q}\hat{\Lambda}\hat{Q}^{-1}$$

where

$$\hat{A} = \begin{pmatrix} \hat{r}w_{11} \ldots \hat{r}w_{1N} & \hat{r}w_{21} \ldots \hat{r}w_{2N} & \ldots \hat{r}w_{M1} \ldots \hat{r}w_{MN} \\ \hat{g}_{11} \ldots \hat{g}_{1N} & \hat{g}_{21} \ldots \hat{g}_{2N} & \ldots \hat{g}_{M1} \ldots \hat{g}_{MN} \\ \hat{b}_{11} \ldots \hat{b}_{1N} & \hat{b}_{21} \ldots \hat{b}_{2N} & \ldots \hat{b}_{M1} \ldots \hat{b}_{MN} \end{pmatrix},$$

$$\hat{Q} = \begin{pmatrix} \hat{q}_{11} & \hat{q}_{12} & \hat{q}_{13} \\ \hat{q}_{21} & \hat{q}_{22} & \hat{q}_{23} \\ \hat{q}_{31} & \hat{q}_{32} & \hat{q}_{33} \end{pmatrix}, \qquad \hat{\Lambda} = \begin{pmatrix} \hat{\lambda}_{11} & 0 & 0 \\ 0 & \hat{\lambda}_{22} & 0 \\ 0 & 0 & \hat{\lambda}_{33} \end{pmatrix}$$

and $\hat{\lambda}_{11} \geq \hat{\lambda}_{22} \geq \hat{\lambda}_{33}$.

The principle components of matrix $\hat{C}$ are written as

$$\hat{P}_w = \begin{pmatrix} \hat{P}w_r \\ \hat{P}_g \\ \hat{P}_b \end{pmatrix} = \hat{Q}^T\hat{A} = \begin{pmatrix} \hat{p}rw_{11} \ldots \hat{p}rw_{1N} & \hat{p}rw_{21} \ldots \hat{p}rw_{2N} & \ldots \hat{p}rw_{M1} \ldots \hat{p}rw_{MN} \\ \hat{p}g_{11} \ldots \hat{p}g_{1N} & \hat{p}g_{21} \ldots \hat{p}g_{2N} & \ldots \hat{p}g_{M1} \ldots \hat{p}g_{MN} \\ \hat{p}b_{11} \ldots \hat{p}b_{1N} & \hat{p}b_{21} \ldots \hat{p}b_{2N} & \ldots \hat{p}b_{M1} \ldots \hat{p}b_{MN} \end{pmatrix}.$$

Let the matrix

$$\hat{P}rnw = \begin{pmatrix} \hat{p}rw_{11} & \hat{p}rw_{12} & \ldots & \hat{p}rw_{1N} \\ \hat{p}rw_{21} & \hat{p}rw_{22} & \ldots & \hat{p}rw_{2N} \\ \vdots & \vdots & \ddots & \vdots \\ \hat{p}rw_{M1} & \hat{p}rw_{M2} & \ldots & \hat{p}rw_{MN} \end{pmatrix}$$

be decomposed into its sub-bands using DWT as follows

$$\begin{aligned} \left(\hat{LL}_1\ \hat{LH}_1\ \hat{HL}_1\ \hat{HH}_1\right) &= DWT(\hat{P}_{rnw}), \\ \left(\hat{LL}_2\ \hat{LH}_2\ \hat{HL}_2\ \hat{HH}_2\right) &= DWT(\hat{LL}_1). \end{aligned}$$

Let us decompose second level sub-bands as follows

$$\begin{aligned} \hat{LL}_2 &= \hat{U}_1\hat{S}_1\hat{V}_1^T, \\ \hat{LH}_2 &= \hat{U}_2\hat{S}_2\hat{V}_2^T, \\ \hat{HL}_2 &= \hat{U}_3\hat{S}_3\hat{V}_3^T, \\ \hat{HH}_2 &= \hat{U}_4\hat{S}_4\hat{V}_4^T. \end{aligned}$$

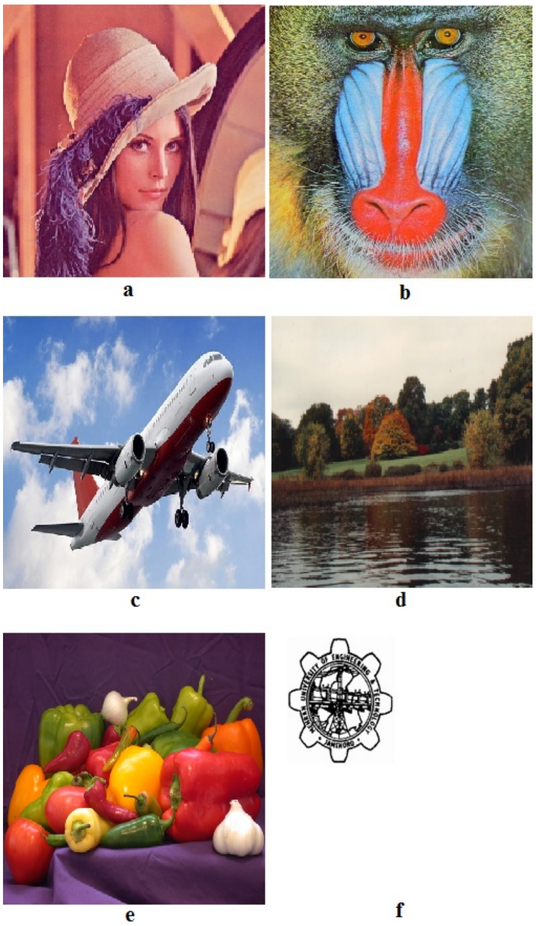

Fig. 1. (a) Lena, (b) Baboon, (c) Aeroplane, (d) Autumn, (e) Peppers (f) Watermark(logo).

Watermarks extracted are

$$W_{LL} = \frac{U_{w1}\hat{S}_1 V_{w1}^T - S_1}{\alpha},$$
$$W_{LH\&HL} = \frac{U_{w2}\hat{S}_2 V_{w2}^T - S_2}{\alpha} + \frac{U_{w3}\hat{S}_3 V_{w3}^T - S_3}{\alpha},$$
$$W_{HH} = \frac{U_{w4}\hat{S}_4 V_{w4}^T - S_4}{\alpha}.$$

Remark 8: There are three watermarks W_{LL} extracted from LL band, W_{HH} from HH band and $W_{LH\&HL}$ extracted from LH and HL band. The watermark $\hat{W}$ with highest NC is the extracted watermark (out of W_{LL}, W_{HH}, and $W_{LH\&HL}$).

3. Experimental Result

Various experiments were performed to explore the consequences of embedding and extraction of watermark into the color images. For this purpose, color images of size (512×512) and gray watermark (logo) (128×128) were chosen as shown in Fig. 1. Haar wavelet is used for comparison.

Perceptual imperceptibility (quality of watermarked image [6], [20]) is measured by PSNR [3], [12], and robustness (similarity of original watermark with extracted watermark [3], [5]) is measured via NC.

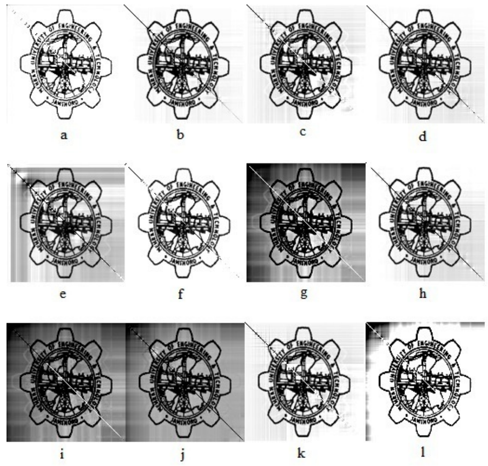

Fig. 2. (a) Histogram Equalization, (b) Rotation, (c) Gaussian Noise, (d) Scaling, (e) Cropping, (f) Y-shearing, (g) X-shearing, (h) Median Filtering, (i) Affine Transformation, (j) Translation, (k) Salt & Pepper, (l) Sharpening.

Attacks	1^{st} Level	2^{nd} Level	3^{rd} Level
Histogram Equalization	0.8217	0.8381	0.5802
Rotation	0.8045	0.8534	0.8892
Gaussian Noise	0.7894	0.8287	0.8211
Scaling	0.7345	0.8393	0.8776
Cropping	0.5625	0.4918	0.6099
Y-Shearing	0.8196	0.8431	0.8607
X-Shearing	0.8309	0.8358	0.7545
Median Filtering	0.7067	0.8307	0.8846
Affine Transformation	0.8218	0.8412	0.7487
Translation	0.8487	0.8968	0.7620
Salt & Pepper	0.7803	0.8227	0.8122
Sharpening	0.8279	0.8578	0.9296

Tab. 1. NCs for different levels ($\alpha = 0.3$).

$$\mathrm{PSNR(dB)} = 10\log_{10}\left(\frac{G^2}{\frac{1}{M\times N}\sum_{m=1}^{M}\sum_{n=1}^{N}(I(m,n)-I_w(m,n))^2}\right)$$

where G is the maximum possible intensity value,

$$NC = \frac{\sum_{k=1}^{K}\sum_{l=1}^{L}\left(W(k,l)\times\hat{W}(k,l)\right)}{\sqrt{\sum_{k=1}^{K}\sum_{l=1}^{L}W^2(k,l)}\sqrt{\sum_{k=1}^{K}\sum_{l=1}^{L}\hat{W}^2(k,l)}}.$$

Various attacks (histogram equalization, rotation, Gaussian noise, scaling, cropping, Y-shearing, X-shearing, median filtering, affine transformation, translation, salt & pepper, and sharpening) were applied on watermarked image to evaluate the performance of purposed scheme. The extracted watermarks are shown in Fig.2.

The results in terms of NC for different level of DWT decomposition are shown in Tab. 1 (using Lena image).

Images	1^{st} Level	2^{nd} Level	3^{rd} Level
Lena	55.6232	66.8290	70.9174
Baboon	42.6506	66.8290	68.1598
Aeroplane	54.3406	63.1777	78.3717
Autumn	50.3772	71.1457	69.7282
Peppers	51.1524	62.1909	67.8758

Tab. 2. PSNR for different levels ($\alpha = 0.3$).

Images	α (0.03)	α (0.05)	α (0.1)	α (0.3)	α (0.5)	α (0.7)	α (0.9)
Lena	93.109	91.773	81.313	66.829	62.999	59.499	56.114
Baboon	99.306	86.369	77.949	66.829	53.014	49.799	48.809
Aeroplane	99.106	98.057	84.535	63.178	62.019	59.374	56.110
Autumn	89.164	81.798	74.773	71.146	58.610	55.169	51.975
Peppers	92.616	84.583	75.046	62.191	57.625	54.649	53.060

Tab. 3. PSNR for different α.

Attacks	α (0.03)	α (0.05)	α (0.1)	α (0.3)	α (0.5)	α (0.7)	α (0.9)
Histogram Equalization	0.268	0.375	0.600	0.838	0.833	0.815	0.822
Rotation	0.968	0.961	0.937	0.853	0.814	0.799	0.780
Gaussian Noise	0.417	0.616	0.792	0.829	0.836	0.840	0.833
Scaling	0.761	0.849	0.891	0.839	0.791	0.782	0.770
Cropping	0.273	0.273	0.273	0.492	0.585	0.616	0.624
Y-Shearing	0.760	0.890	0.875	0.843	0.827	0.811	0.794
X-Shearing	0.505	0.665	0.811	0.836	0.837	0.824	0.809
Median Filtering	0.612	0.417	0.846	0.831	0.776	0.746	0.742
Affine Transformation	0.517	0.640	0.743	0.841	0.848	0.836	0.821
Translation	0.701	0.751	0.895	0.897	0.862	0.8379	0.819
Salt & Pepper	0.400	0.340	0.773	0.823	0.843	0.8392	0.826
Sharpening	0.263	0.271	0.519	0.858	0.848	0.8268	0.824

Tab. 4. NC for different α.

The results in terms of PSNR for different level of DWT decomposition are shown in Tab. 2 (using different images).

Note that, with increase in level, the imperceptibility improves. Therefore, we use second level DWT for following simulations.

The performance of the proposed scheme in terms of PSNR is shown in Tab. 3 (using different images), and in terms of NC is shown in Tab. 4 (using Lena image), for different strength factors (i.e. α).

It is clear from the values that larger strength factor provides better robustness while a smaller strength factor gives good imperceptibility results. Different images are also used to measure the quality of proposed scheme and the result is shown in Tab. 5.

Tab. 6 and Tab. 7 show the comparison of the proposed scheme with different schemes in terms of NC and PSNR respectively (for Lena image). It is obvious from the result that our scheme performs well.

Attacks	Lena	Baboon	Aeroplane	Autumn	Peppers
Histogram Equalization	0.8381	0.8353	0.8152	0.8166	0.8072
Rotation	0.8534	0.8532	0.8330	0.8607	0.8407
Gaussian Noise	0.8287	0.8274	0.8130	0.8111	0.7903
Scaling	0.8393	0.8392	0.8174	0.8452	0.8305
Cropping	0.4918	0.4903	0.2966	0.2749	0.4091
Y-Shearing	0.8431	0.8408	0.7906	0.8316	0.7883
X-Shearing	0.8358	0.8333	0.8154	0.8335	0.7845
Median Filtering	0.8307	0.8306	0.8045	0.8256	0.8181
Affine Transform	0.8412	0.8387	0.8164	0.7932	0.8059
Translation	0.8968	0.8953	0.9001	0.8429	0.8202
Salt & Pepper	0.8227	0.8211	0.7954	0.8209	0.8152
Sharpening	0.8578	0.8573	0.9054	0.8881	0.9052

Tab. 5. NCs for different images ($\alpha = 0.3$).

Attacks	Proposed scheme	DWT-SVD based [13]	DWT [15]	SVD [16]
Histogram Equalization	0.8381	0.6111	0.1453	0.2235
Rotation	0.8534	0.2404	0.2372	0.3080
Gaussian Noise	0.8287	0.6050	0.2053	0
Scaling	0.8393	0.2415	0.2369	0.3080
Cropping	0.4918	0.2397	0.2493	0.2051
Y-Shearing	0.8431	0.2396	0.1999	0.2164
X-Shearing	0.8358	0.5836	0.2148	0.2588
Median Filtering	0.8307	0.5249	0.8191	0.2923
Affine Transformation	0.8412	0.5162	0.2439	0.2263
Translation	0.8968	0.2320	0.2103	0.1917
Salt & Pepper	0.8227	0.6028	0.4179	0
Sharpening	0.8578	0.6587	0.8457	0.3052

Tab. 6. NC for different Schemes

Image	Proposed scheme	DWT-SVD based [13]	DWT [15]	SVD [16]
Lena	66.8290	5.1733	42.8330	34.2224

Tab. 7. PSNR for different schemes.

4. Conclusion

A PCA-DWT-SVD based non-blind watermarking scheme is proposed. In this scheme all DWT sub-bands are chosen for watermark embedding, therefore it is very difficult to remove the watermark. The proposed scheme is tested using different strength factors and using different images and it is found that this scheme performs well against many attacks (including histogram equalization, rotation, Gaussian noise, scaling, cropping, Y-shearing, X-shearing, median filtering, affine transformation, translation, salt & pepper, and sharpening). Since imperceptibility and robustness are the measure for quality of watermark the results show that this scheme satisfies both quality measures.

References

[1] YIN, C.-Q., LI, L., LV, A.-Q., QU, L. A color image watermarking algorithm based on DWT-SVD. In *IEEE Internation Conference on Automation and Logistics.* Jinan (China), 2007, p. 2607 - 2611.

[2] GANIC, E., ESKICIOGLU, A. M. Robust DWT-SVD domain image watermarking: Embedding data in all frequencies. In *Proceedings of the 2004 Workshop on Multimedia and Security.* Magdeburg (Germany), 2004, p. 166 - 174.

[3] SANTHI, V., REKHA, N., THARINI, S. A hybrid block based watermarking algorithm using DWT-DCT-SVD techniques for color images. In *International Conference on Computing, Communication and Networking, ICCCn.* St. Thomas (USA), 2008, p. 1 - 7.

[4] LAI, C. C., TSAI, C. C. Digital image watermarking using discrete wavelet transform and singular value decomposition. *IEEE Transactions on Instrumentation and Measurement,* 2010, vol. 59, no. 11, p. 3060 - 3063.

[5] DHARWADKAR, N. V., AMBERKER, B. B., GORAI, A. Non-blind watermarking scheme for color images in RGB space using DWT-SVD. In *International Conference on Communications and Signal Processing (ICCSP).* Calicut (India), 2011, p. 489 - 493.

[6] BHAGYASHRI, S. K., JOSHI, M. Y. All frequency band DWT-SVD robust watermarking technique for color images in YUV color space. In *IEEE Conference on Computer Science and Automation Engineering (CSAE).* Shanghai (China), 2011, p. 295 - 299.

[7] ZHANG, H., SHU, H., COATRIEUX, G., ZHU, J., WU, Q. M. J., ZHANG, Y., ZHU, H., LUO, L. Affine Legendre Moment Invariants for image watermarking robust to geometric distortions. *IEEE Transactions on Image Processing,* 2011, vol. 20, no. 8, p. 2189 - 2199.

[8] SONG, H., QIU, Z., GU, J. A novel semi-fragile image watermarking scheme based on wavelet. In *IEEE International Conference on Audio Language and Image Processing (ICALIP).* Shanghai (China), 2010, p. 1504 - 1510.

[9] RAWAT, S., RAMAN, B. A new robust watermarking scheme for color images. In *IEEE 2nd International Advance Computing Conference.* Patalia (India), 2010, p. 206 - 209.

[10] AGARWAL, R., SANTHANAM, M. S., VENUGOPALAN, K. Multichannel digital watermarking of color images using SVD. In *IEEE International Conference on Image Information Processing.* Waknaghat (India), 2011, p.1 - 6.

[11] BHATNAGAR, G., RAMAN, B. A new robust reference watermarking scheme based on DWT-SVD. *International Journal of Computer Standards & Interfaces*, 2009, vol. 31, no. 5, p. 1002 - 1013.

[12] SANTHI, V., THANGAVELU, A. DWT-SVD combined full band robust watermarking technique for color images in YUV color space. *International Journal of Computer Theory and Engineering*, 2009, vol. 1, no. 4, p. 1793 - 8201.

[13] GUNJAL, B. L., MALI, S. N. Comparative performance analysis of DWT-SVD based color image watermarking technique in YUV, RGB and YIQ color spaces. *International Journal of Computer Theory and Engineering*, 2011, vol. 3, no. 6, p. 714 - 717.

[14] KAPOOR, P., SHARMA, K. K., BEDI, S. S., KUMAR, A. Colored image watermarking technique based on HVS using HSV color model. In *In Proceedings of International Conference on Advances in Computer Engineering.* Trivandrum (India), 2011, pp. 20-24.

[15] KHALIFA, A., HAMMAD, S. A robust non-blind algorithm for watermarking color images using multi-resolution wavelet decomposition. *International Journal of Computer Applications*, 2012, vol. 37, no. 8, p. 33 - 39.

[16] XING, Y., TAN, J. A color image watermarking scheme resistant against geometrical attacks. *Radioengineering*, 2010, vol. 19, no. 1, p. 62 - 47.

[17] SUN, X., BO, S. A blind digital watermarking for color medical images based on PCA. In *IEEE International Conference on Wireless Communications, Networking and Information Security (WCNIS).* Beijing (China), 2010, p. 421 - 427.

[18] JOLLIFFE, I. T. Introduction. *Principle Component Analysis,* 2nd ed. New York: Springer, 2002, p. 1 - 6.

[19] YANAI, H., TAKEUCHI, K., TAKANE, Y. Singular value decomposition. *Projection Matrices, Generalized Inverse Matrices, and Singular Value Decomposition,* 1st ed. New York: Springer, 2011, p. 125 - 148.

[20] LAI, C. C. An improved SVD-based watermarking scheme using human visual characteristics. *International Journal of Optics Communications*, 2011, vol. 284, no. 4, p. 938 - 944.